



Molecular Crystals and Liquid Crystals

Publication details, including instructions for authors and subscription information:

<http://www.tandfonline.com/loi/gmcl20>

Discrete Light Propagation and Self-Localization in Voltage-Controlled Arrays of Channel Waveguides in Undoped Nematic Liquid Crystals

Andrea Fratalocchi^a, Gaetano Assanto^a, Katarzyna A. Brzdąkiewicz^b & Mirosław A. Karpierz^b

^a NooEL - Nonlinear Optics and Optoelectronics Laboratory, Italian Institute for Physics of Matter and CNISM, Department of Electronic Engineering, University "Roma Tre", Rome, Italy

^b Faculty of Physics, Warsaw University of Technology, Warsaw, Poland

Version of record first published: 22 Sep 2006

To cite this article: Andrea Fratalocchi, Gaetano Assanto, Katarzyna A. Brzdąkiewicz & Mirosław A. Karpierz (2006): Discrete Light Propagation and Self-Localization in Voltage-Controlled Arrays of Channel Waveguides in Undoped Nematic Liquid Crystals, *Molecular Crystals and Liquid Crystals*, 453:1, 191-202

To link to this article: <http://dx.doi.org/10.1080/15421400600654033>

PLEASE SCROLL DOWN FOR ARTICLE

Full terms and conditions of use: <http://www.tandfonline.com/page/terms-and-conditions>

This article may be used for research, teaching, and private study purposes. Any substantial or systematic reproduction, redistribution, reselling, loan, sub-licensing, systematic supply, or distribution in any form to anyone is expressly forbidden.

The publisher does not give any warranty express or implied or make any representation that the contents will be complete or accurate or up to date. The accuracy of any instructions, formulae, and drug doses should be independently verified with primary sources. The publisher shall not be liable for any loss, actions, claims, proceedings, demand, or costs or damages whatsoever or howsoever caused arising directly or indirectly in connection with or arising out of the use of this material.

Discrete Light Propagation and Self-Localization in Voltage-Controlled Arrays of Channel Waveguides in Undoped Nematic Liquid Crystals

Andrea Fratalocchi

Gaetano Assanto

NooEL - Nonlinear Optics and Optoelectronics Laboratory, Italian
Institute for Physics of Matter and CNISM, Department of Electronic
Engineering, University “Roma Tre”, Rome, Italy

Katarzyna A. Brzdąkiewicz

Mirosław A. Karpierz

Faculty of Physics, Warsaw University of Technology, Warsaw, Poland

We review linear and nonlinear light propagation in a voltage-tunable liquid crystalline waveguide array. We report on discrete diffraction, discrete soliton generation, all-optical beam steering, multiband vector breathers and Bloch oscillations. The predictions, based on full numerical BPM simulations, are in excellent agreement with the experimental results.

Keywords: all-optical beam steering; Bloch oscillations; discrete propagation; liquid crystals waveguide arrays; spatial solitons; vector breathers

1. INTRODUCTION

Linear and nonlinear light propagation in one dimensional arrays of optical waveguides have been the subject of intensive investigations in recent years. Stemming from the pioneering work by Somekh *et al.* [1] (who experimentally demonstrated linear tunneling in a one dimensional optical lattice), by Jensen [1] (on the nonlinear directional coupler), and by Christodoulides and Joseph [2] (on an infinite array of

The samples were generously provided by E. Nowinowski-Kruszelnicki.

Address correspondence to Gaetano Assanto, NooEL - Nonlinear Optics and Optoelectronics Laboratory, Italian Institute for Physics of Matter and CNISM, Department of Electronic Engineering, University “Roma Tre”, Via della Vasca Navale 84, 00146 Rome, Italy. E-mail: assanto@uniroma3.it

identical waveguides), several studies have been pursued exploiting various materials and nonlinearities [3–16]. An optical lattice, in most cases, can be simply described using coupled mode theory (CMT), which models light propagation in terms of guided modes evanescently coupled to neighboring channels [2]. The generation of localized states (i.e., discrete solitons) can be therefore understood as resulting from the balance between discrete diffraction (owing to waveguides coupling) and the nonlinearly induced refractive index shift, which detunes a finite number of waveguides from the others, favoring light localization. Quite interestingly, such mechanism results in lowering the optical power requirement for light localization as compared to their continuous counterparts (i.e., spatial solitons). In the latter cases, in fact, a “nonlinear” waveguide needs to be entirely created, while in the former just a small (phase) detuning suffices [3]. Discrete solitons have been experimentally reported in AlGaAs [6–7], silica [8–9], Lithium Niobate [12], SBN-crystals [13–15] and liquid crystals [16]. All-optical switching and readdressing have been proposed and successfully demonstrated in such materials [16–22,44].

As for photonic crystals or electrons in periodic structures [23], a more accurate analysis would require the use of Bloch theory, paving the way to the observation of gap solitons [24,25], discrete breathers [26,27], multiband vector solitons [16–30] and dynamics typical of quantum-mechanical systems such as Bloch oscillations [31–35] and tunneling in an “accelerated” lattice [36].

Undoped nematic liquid crystals (NLC) are excellent materials for nonlinear optics [37–45]. Among their several advantages, we mention their giant non-resonant nonlinearity, their inexpensive and mature technology, their huge birefringence and low power requirements for light localization (few mW), allowing the observation of spatial solitons with propagation distances of millimeters [16,40–45]. In addition, the large electro-optic response of NLC entails flexible and voltage-tunable architectures [16]. This bias-controlled flexibility, at variance with solid-state waveguide arrays, permits the precise adjustment of individual waveguide channels as well as their mutual coupling both in linear and nonlinear regimes.

This article is organized as follows. In Section 2 we describe the NLC cell geometry, a voltage-controlled array of identical channel waveguides in undoped nematic liquid crystals. In Section 3 we summarize both model and experiments on discrete light propagation and self-confinement (discrete diffraction, discrete solitons, angular steering and Bloch oscillations). In Section 4 we introduce a more rigorous treatment based on Bloch mode expansion, and discuss a novel type of localization.

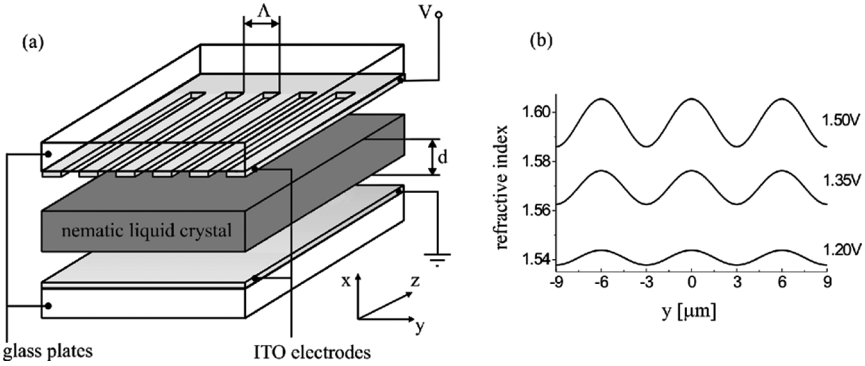


FIGURE 1 (a) Sketch of the voltage-controlled liquid crystalline waveguide array; (b) refractive index in the cell midpoint versus bias in a cell with $d = 5 \mu\text{m}$, $\Lambda = 3 \mu\text{m}$.

2. A WAVEGUIDE ARRAY IN NEMATIC LIQUID CRYSTALS

The sample is sketched in Figure 1a. A thin layer of 5CB (of thickness d) is placed between two glass plates, forming a planar waveguide in the absence of an applied voltage. The anchoring conditions provided by the glass interfaces force the planar alignment of NLC molecules along the z -direction (corresponding to light propagation). An array of parallel transparent indium-tin-oxide electrodes (with identical width and spacing) is employed to introduce a spatially periodic modulation of the refractive index across the cell. The application of a proper low-frequency bias, in fact, induces reorientation of the NLC molecules which, due to self-energy minimization, change their angle θ with respect to z , i.e., the direction of their optic axis. The latter rotation, owing to the periodic spatial distribution of the applied field, gives rise to a periodic (extraordinary) refractive index modulation across the sample and therefore defines an array of identical channel waveguides supporting TM-polarized guided modes [16]. The director distribution θ can be calculated using Frank's free energy formulation and the Euler-Lagrange Equations [35–37]. Typical distributions of refractive index versus bias, calculated in the cell midpoint, are displayed in Figure 1b.

3. DISCRETE LIGHT PROPAGATION

3.1. Discrete Diffraction and Discrete Solitons

Numerical simulations of light propagating (Fig. 2) in the NLC array were performed using a nonlinear beam propagation (BPM) code [16].

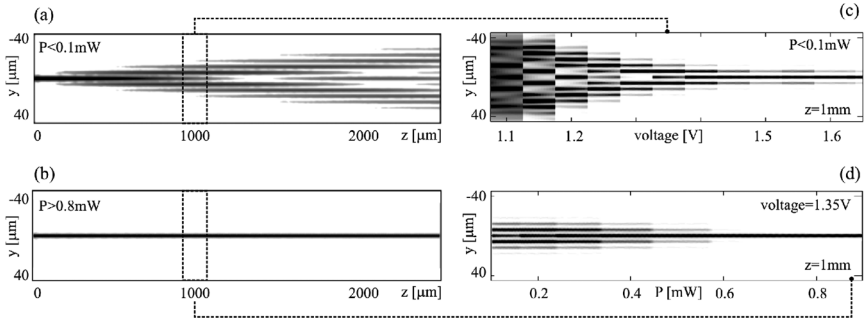


FIGURE 2 Linear and nonlinear BPM simulation of a Gaussian beam propagating ($w = 2 \mu\text{m}$) in the NLC array ($d = 5 \mu\text{m}$, $\Lambda = 6 \mu\text{m}$): (a) discrete diffraction at $P < 0.1 \text{ mW}$; (b–c) sections of light propagation versus applied voltage (b) and input power (c); (d) discrete soliton generation for $P > 0.8 \text{ mW}$.

At the input, a TM-polarized Gaussian beam of wavelength $\lambda = 1064 \text{ nm}$ was launched. At this wavelength 5CB has refractive indices $n_o = 1.52$ and $n_e = 1.69$ and low-frequency electric anisotropy $\Delta\epsilon_{lf} = 11.5$. In the linear regime, at input powers $P < 0.1 \text{ mW}$, light tunnels from waveguide to waveguide via evanescent coupling, spreading among channels and originating the characteristic pattern known as discrete diffraction (Fig. 2a) [42]. The tunneling process can be adjusted by acting on the external bias, as displayed in Figure 2b. As the voltage increases, in fact, reorientation gets stronger in the waveguide-core regions¹ and, due to better confinement, light transfers energy over longer coupling distances.

As the input power increases, it can reorient the liquid crystals and induce a refractive index change [42]. As displayed in Figure 2c–d, the coupling process becomes less and less efficient with self-focusing. The nonlinearly induced index increase, in fact, mismatches nearby waveguides which were perfectly *resonant* in the linear regime, thereby favoring light self-localization. When discrete diffraction is perfectly balanced by the nonlinearity, all energy coupled into the cell propagates without spreading and a localized state, known as *discrete soliton*, appears (Fig. 3d). This intuitive picture – based on coupled mode theory – can be retrieved with a more rigorous treatment which also accounts for non locality in NLC [43].

Experiments were carried out in NLC cells of thickness $d = 6 \mu\text{m}$ and electrode period $\Lambda = 8 \mu\text{m}$. A near infrared ($\lambda = 1.064 \mu\text{m}$) Nd:YAG laser beam was focused into the sample and the light scattered out of the

¹As explained in Sec. 4.1, this is valid up to a specified threshold.

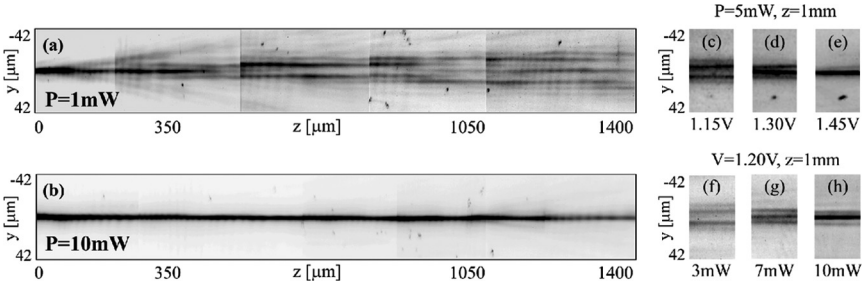


FIGURE 3 Experimental results on discrete light propagation in an NLC cell ($d=5\text{ }\mu\text{m}$, $\Lambda=6\text{ }\mu\text{m}$) with $V=0.74\text{ V}$: (a) linear diffraction for $P=1\text{ mW}$; (b) discrete soliton propagation for $P=10\text{ mW}$; (c–h) sections of light evolution in $z=1.4\text{ mm}$ versus voltage (c–e) and input power (f–h).

(y-z) plane acquired by an optical microscope and a high resolution CCD camera. Figure 3 displays discrete light propagation in an array defined by a bias of 0.74 V . For low optical power ($P=1\text{ mW}$), discrete diffraction takes place in perfect agreement with both coupled mode theory and our numerical simulations. As the voltage increases for a constant input power, discrete diffraction decreases in magnitude due to better light confinement in the channels (Fig. 3b). Conversely, when the input power increases ($P=10\text{ mW}$) for a fixed bias, a discrete soliton is formed (as self-focusing mismatches the launch waveguide) and propagates straight without any transverse coupling (Fig. 3c–d).

3.2. Nonlinear Beam Steering

A quite remarkable property of periodic arrays stems from their lack of rotational symmetry. While in free space or in a continuous bulk medium light can propagate at every angle, in a waveguide array, conversely, if a finite number of channels confines the excitation via self-focusing the energy does not *feel* the neighboring channels and propagates straight, regardless the launch angle or tilt. In other terms, light can obliquely cross a photonic array in the linear regime but, above a certain power threshold, it self-confines and propagates parallel to the waveguide axis. Such a power dependent – hence *nonlinear* – *beam steering* offers interesting possibilities for all-optically switching and routing of optical signals [5].

Discrete beam steering can be analyzed in NLC using a nonlinear BPM-code. At the input, a Gaussian beam of waist $\omega=10\text{ }\mu\text{m}$

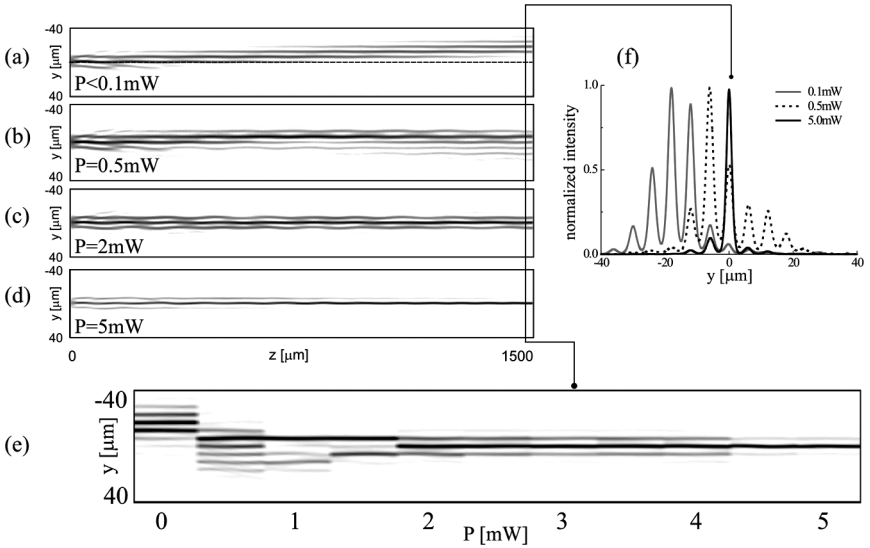


FIGURE 4 Numerical experiments on Gaussian beam propagation ($w_{0x} = 2 \mu\text{m}$, $w_{0y} = 10 \mu\text{m}$) tilted of 1.90° along y : (a–d) nonlinear beam steering versus power $0.1 < P < 7 \text{ mW}$ ($V = 1.35$); (e–f) output intensities section (e) and transverse beam profiles in $z = 1.5 \text{ mm}$ (f) versus input power P ($V = 1.35$).

is injected into a NLC cell of thickness $d = 5 \mu\text{m}$ and electrode period $\Lambda = 6 \mu\text{m}$ with an initial tilt of about 1.90° along y . The latter corresponds to the condition of minimum diffraction (maximum transverse velocity along y). In the linear regime ($P < 0.1 \text{ mW}$) light obliquely moves across the array as in Figure 4a. As the power increases, however, light starts reorienting the liquid crystal molecules and therefore reduces its transverse velocity thru nonlinear detuning. Finally, for high enough input powers ($P = 7 \text{ mW}$), the input waveguide is completely mismatched in the array and light propagates straight (Fig. 4b–f). Our experimental results are displayed in Figure 5 for a bias $V = 0.77 \text{ V}$. Discrete diffraction can be observed at a low power $P = 1 \text{ mW}$ (Fig. 5a), whereas light localizes in a single channel as $P = 7 \text{ mW}$ (Fig. 5b). Nonlinear beam steering is clearly visible in Figure 5c, showing the output intensity distributions for various input powers, as well as in Figure 5d which graphs the output transverse intensity profiles. Such effect has potential applications in all-optical switching, steering and multipoint routing [44].

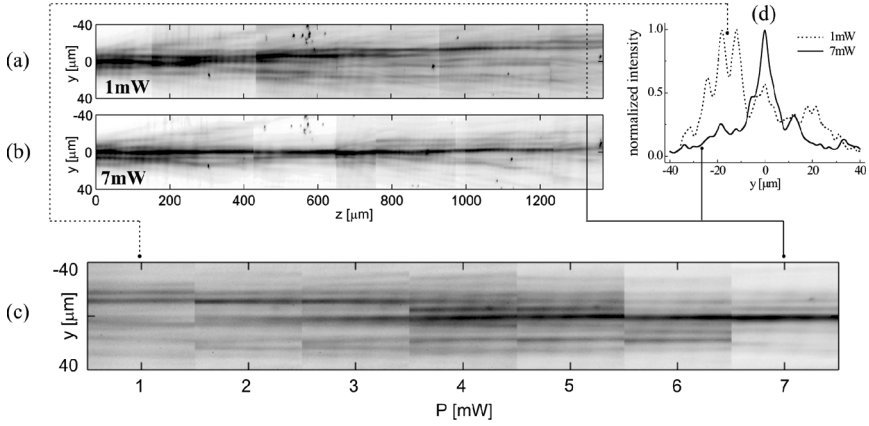


FIGURE 5 Experimental results on nonlinear beam steering employing an input gaussian beam ($w_{0x} = 2 \mu\text{m}$, $w_{0y} = 10 \mu\text{m}$) tilted of 1.90° along y , in an array defined by $V = 0.77 V$: (a) discrete propagation ($P = 1 \text{ mW}$); (b) beam steering at $P = 7 \text{ mW}$; (c) output light intensity distribution versus input power as in (d) for two specific excitations.

3.3. Bloch Oscillations

As discussed in literature, Bloch oscillations (BO) can be observed in a photonic lattice provided a linear gradient of its transverse index distribution is available [31–35]. Hence, with reference to liquid crystalline waveguide arrays, BO could be obtained in several ways as various parameters of the structure can be easily modified. The applied voltage could be linearly altered from one stripe electrode to the next, the temperature could be ramped across the array, the cell could be shaped into a (transverse) wedge. We address the latter possibility, making the NLC thickness a linear function of the transverse y coordinate, i.e., $d = d_0 + \eta y$.

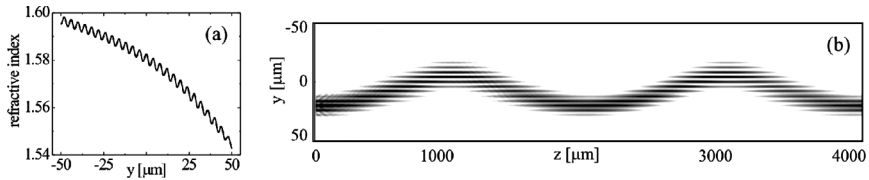


FIGURE 6 (a) Refractive index along y in cell midpoint of a NLC ($V = 1.3 V$, $\Lambda = 4 \mu\text{m}$). The thickness slope was taken as $\beta = 56^\circ$, with β the angle between the glass surface and the y direction. (b) Linear BPM simulation of Bloch oscillations for a Gaussian input beam ($\omega = 10 \mu\text{m}$).

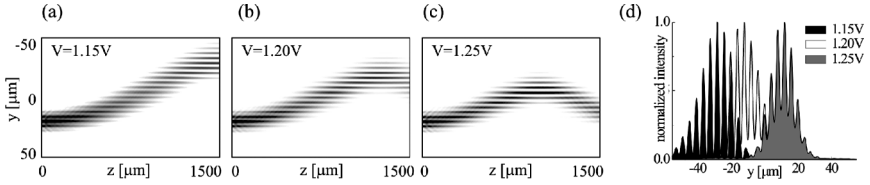


FIGURE 7 (a–c) Bloch oscillations and output intensity sections (d) versus applied voltage for a gaussian input ($w = 10\ \mu\text{m}$) and a cell with $V = 1.3\text{ V}$, $\Lambda = 4\ \mu\text{m}$.

Figure 6a is an example of refractive index distribution obtained in the middle of an NLC layer forming a wedge of slope $56'$, for an electrode period $\Lambda = 4\ \mu\text{m}$. Due to the thickness change, a linear gradient is added to the periodic refractive modulation, resulting in slight differences between the optical parameters of neighboring channels. In such an array, linear light propagation results into Bloch oscillations, as in Figure 6b for an input Gaussian beam of waist $w = 10\ \mu\text{m}$ (broad excitation) launched parallel to the z -axis. Light oscillates periodically in the transverse direction, such cyclic behavior depending on the periodic nature of the eigenmodes, known as Wannier-Stark states [32]. Moreover, in NLC arrays both BO amplitude and period can be controlled by acting on the applied voltage. Figure 7a–c show calculated BO period versus bias. As the latter increases, the linear gradient (added to the periodic index profile) increases as well and the oscillation period decreases. Since the output beam position can be adjusted and controlled (Fig. 7d), this effect has potential applications in signal switching and readdressing schemes.

4. NLC LATTICE DYNAMICS

4.1. Multiband Breathers

Coupled mode theory predicts various phenomena related to the eigenmodes of a single channel. A more rigorous and complete treatment of the lattice dynamics, however, requires an expansion in Floquet-Bloch (FB) modes and the calculation of the array eigenvalue spectrum, relating propagation constant k_z to the Bloch wave number K_y [23]. Figure 8a shows the numerically calculated dispersion diagram of an NLC array with $d = \Lambda = 6\ \mu\text{m}$, filled with standard 5CB and with an applied bias $V = 0.9\text{ V}$. The spectrum is composed by linear FB bands separated by gaps, hence it is much richer than the simple picture of an upper sinusoidal band with a semi-infinite gap, as provided

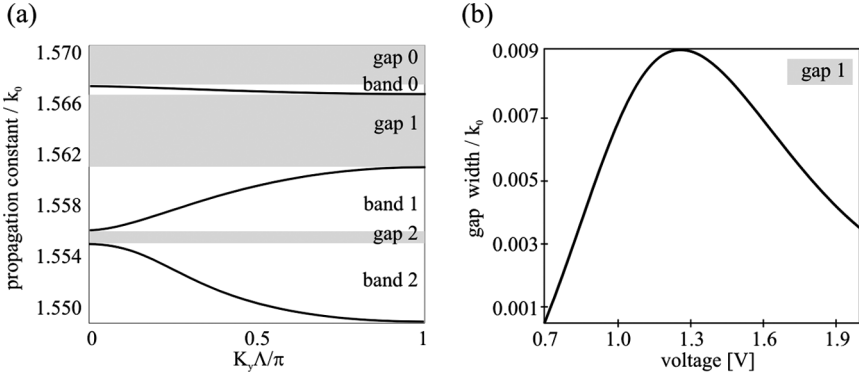


FIGURE 8 (a) Band-gap diagram for an NLC array with $d = \Lambda = 6 \mu\text{m}$ and an applied voltage of 0.9 V; (b) width of gap 1 versus voltage.

by CMT [46]. Quite interestingly, since the dispersion depends on the refractive index and the latter can be electro-optically adjusted in NLC, each band/gap in the spectrum can be tuned by acting on the external bias [45]. The system effectively behaves as a tunable 1D photonic lattice. Figure 8b displays the tuning of the first gap versus bias. The gap width increases with applied voltage ($V < 1.3 \text{ V}$) up to a maximum, then r ($V > 1.3 \text{ V}$) decreases again once non local and saturating character of NLC reduce the refractive modulation.

A proper superposition of linear FB modes can lead to light localization via cross phase modulation. The resulting light distribution oscillates in a periodic fashion along the direction of propagation z , originating a *multiband optical breather* [45]. Numerical simulations for a superposition of modes in the first two bands are visible in Figure 9, FB modes are not able to self-trap when launched individually (Fig. 9a–d). Band 0 modes (Fig. 9a), with amplitude maxima in the waveguide-core regions, can be excited by a wide Gaussian beam ($P=0.2 \text{ mW}$, $V=1 \text{ V}$) launched in the middle between two channels (Fig. 9c). Band 1 modes possess maxima in-between channels (Fig. 9b) and can be excited by a narrow Gaussian beam ($P=0.2 \text{ mW}$, $V=1 \text{ V}$) centered between waveguides (Fig. 9d). When launched together, the individual modes combine their power and originate a symmetric breather via cross phase modulation, with spatially localized and periodically oscillating propagation (Fig. 9e) [45].

In our experiment we employed a Gaussian beam of waist $w=5 \mu\text{m}$ -centered between two neighboring channels – in an array defined by $\Lambda=6 \mu\text{m}$ and bias $V=1 \text{ V}$. This ensured the adequate excitation of FB modes belonging to the first two bands, with a larger spatial overlap

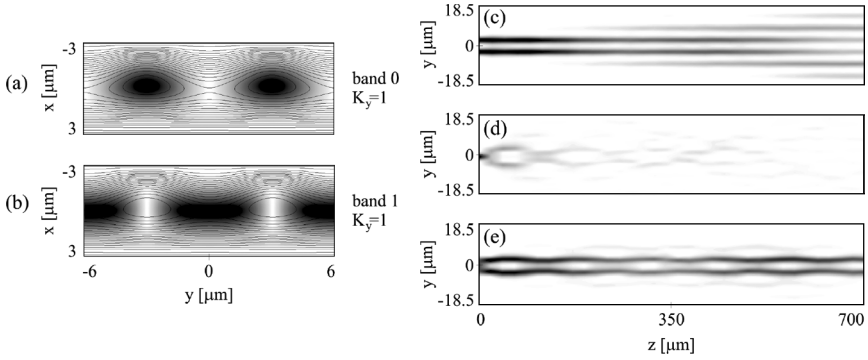


FIGURE 9 FB modal profiles (pseudo-color plot) for $K_y\Lambda/\pi = 1$ in band 0 (a) and in band 1 (b); contour lines correspond to the refractive index distribution. BPM simulations of band 0 (c) and band 1 (d) modes ($P = 0.2$ mW) in an array defined by $V = 1$ V; (e) vector symmetric breather for superimposed excitations (c) and (d).

with the modes belonging to band 1 (due to the input profile). In fact, at low power ($P = 0.2$ mW, Fig. 10a) light evolved as in Figure 9d. As the power was increased, reorientation improved light confinement in the waveguide regions, thereby making the excitation more effective towards modes in band 0 with respect to band 1. When the modes carried equal input powers ($P = 7$ mW), a symmetric breather originated and freely propagated, as in Figure 10b. The period of the breather, depending on the width of the first gap, could be adjusted by acting on the external bias (Fig. 10c), demonstrating once again electro-optic lattice tunability. In agreement with our model, the minimum value of the oscillation period (Fig. 10c) was observed for a voltage close to 1.3 V, which corresponds to the minimum in the first gap width (Fig. 8b).

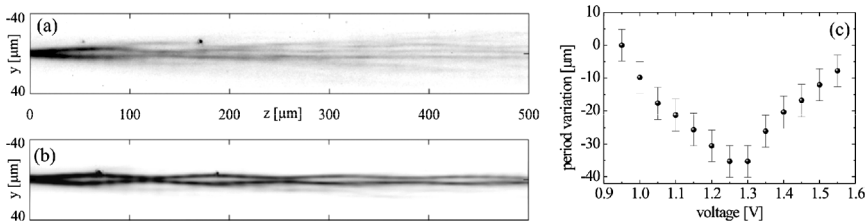


FIGURE 10 Experimental observation of multiband breathers: (a) low ($P = 0.2$ mW) and (b) high power ($P = 7$ mW) light propagation of a Gaussian beam ($w = 5$ μ m) launched in an array defined by $V = 1$ V; (c) breathing period versus bias.

5. CONCLUSIONS

We have investigated, both theoretically numerically and experimentally, discrete light propagation in one-dimensional photonic lattices realized in undoped nematic liquid crystals. The nematic array, at variance with other discrete systems, affords tunability in both linear and nonlinear regimes, thus offering considerable flexibility and an ideal workbench for the investigation of discrete optical phenomena including light localization, nonlinear steering as well as dynamics typical of quantum-mechanics. A large variety of voltage-tunable configurations can be envisioned with potential applications to optical signal processing and multi-functional routers.

REFERENCES

- [1] Somekh, S., Garmire, E., Yariv, A., Garvin, H. L., & Hunsperger, R. G. (1973). *Appl. Phys. Lett.*, 22, 46; Jensen, S. M. (1982). *IEEE J. Quantum Electron.*, QE-18, 1580.
- [2] Christodoulides, D. N. & Joseph, R. I. (1988). *Opt. Lett.*, 13, 794.
- [3] Lederer, F., Darmanyan, S., & Kobayakov, A. (2002). In: *Spatial Solitons*, Trillo, S. & Torruellas, W. (Eds.), Wiley: New York, Chapter 10, 269; Kivshar, Y. S. & Agrawal, G. P. (2003). *Optical Solitons: From Fibers to Photonic Crystals*, Academic Press: New York.
- [4] Sukhorukov, A. A., Kivshar, Y. S., Eisenberg, H. S., & Silberberg, Y. (2003). *IEEE J. Quantum Electron.*, 39, 31.
- [5] Aceves, A. B., De Angelis, C., Peschel, T., Muschall, R., Lederer, F., Trillo, S., & Wabnitz, S. (1996). *Phys. Rev. E*, 53, 1172.
- [6] Eisenberg, H. S., Silberberg, Y., Morandotti, R., & Aitchison, J. S. (2000). *Phys. Rev. Lett.*, 85, 1863–1866.
- [7] Morandotti, R., Eisenberg, H. S., Silberberg, Y., Sohler, M., & Aitchison, J. S. (2001). *Phys. Rev. Lett.*, 86, 3296.
- [8] Cheskis, D., Bar-Ad, S., Morandotti, R., Aitchison, J. S., Eisenberg, H. S., Silberberg, Y., & Ross, D. (2003). *Phys. Rev. Lett.*, 91, 223901.
- [9] Pertsch, T., Peschel, U., Lederer, F., Burghoff, J., Will, M., Nolte, S., & Tunnermann, A. (2004). *Opt. Lett.*, 29, 468.
- [10] Christodoulides, D., Lederer, F., & Silberberg, Y. (2003). *Nature*, 424, 817.
- [11] Etrich, C., Lederer, F., Malomed, B., Peschel, T., & Peschel, U. (2000). In: *Progress in Optics*, Wolf, E. (Ed.), Elsevier Science Publishers, Vol. 41, 483.
- [12] Iwanow, R., Schiek, R., Stegeman, G. I., Pertsch, T., Lederer, F., Min, Y., & Sohler, W. (2004). *Phys. Rev. Lett.*, 93, 113902.
- [13] Efremidis, N. K., Sears, S., Christodoulides, D. N., Fleischer, J. W., & Segev, M. (2002). *Phys. Rev. E*, 66, 046602.
- [14] Fleisher, J. W., Carmon, T., Segev, M., Efremidis, N. K., & Christodoulides, D. N. (2003). *Phys. Rev. Lett.*, 90, 023902.
- [15] Fleisher, J. W., Segev, M., Efremidis, N. K., & Christodoulides, D. N. (2003). *Nature*, 422, 147.
- [16] Fratalocchi, A., Assanto, G., Brzdańiewicz, K. A., & Karpierz, M. A. (2005). *Opt. Expr.*, 13, 1808.
- [17] Krolikowski, W. & Kivshar, Y. S. (1996). *J. Opt. Soc. Am. B*, 13, 876.

- [18] Christodoulides, D. N. & Eugenieva, E. D. (2001). *Phys. Rev. Lett.*, **87**, 233901.
- [19] Pertsch, T., Zentgraf, T., Peschel, U., Brauer, A., & Lederer, F. (2002). *Appl. Phys. Lett.*, **80**, 3247.
- [20] Pertsch, T., Peschel, U., & Lederer, F. (2003). *Opt. Lett.*, **28**, 102.
- [21] Vicencio, R. A., Molina, M. I., & Kivshar, Y. S. (2004). *Phys. Rev. E*, **70**, 026602.
- [22] Bang, O. & Miller, P. D. (1996). *Opt. Lett.*, **21**, 1105.
- [23] Sakoda, K. (2001). *Optical Properties of Photonic Crystals*, Springer: Berlin; Ashcroft, N. W. & Mermin, N. D. (1976). *Solid State Physics*, Saunders College Publishing: New York.
- [24] Mandelik, D., Morandotti, R., Aitchison, J. S., & Silberberg, Y. (2004). *Phys. Rev. Lett.*, **92**, 093904.
- [25] Sukhorukov, A. A. & Kivshar, Y. S. (2003). *Opt. Lett.*, **28**, 2345.
- [26] Flach, S. & Willis, C. R. (1998). *Phys. Rep.*, **295**, 181.
- [27] Mandelik, D., Eisenberg, H. S., Silberberg, Y., Morandotti, R., & Aitchison, J. S. (2003). *Phys. Rev. Lett.*, **90**, 253902.
- [28] Sukhorukov, A. A. & Kivshar, Y. S. (2003). *Phys. Rev. Lett.*, **91**, 113902.
- [29] Cohen, O., Schwartz, T., Fleischer, J. W., Segev, M., & Christodoulides, D. N. (2003). *Phys. Rev. Lett.*, **91**, 113901.
- [30] Desyatnikov, A. S., Ostrovskaya, E. A., Kivshar, Y. S., & Denz, C. (2003). *Phys. Rev. Lett.*, **91**, 153902.
- [31] Morandotti, R., Peschel, U., Aitchison, J. S., Eisenberg, H. S., & Silberberg, Y. (1999). *Phys. Rev. Lett.*, **83**, 4756.
- [32] Peschel, U., Pertsch, T., & Lederer, F. (1998). *Opt. Lett.*, **23**, 1701.
- [33] Pertsch, T., Dannberg, P., Elflein, W., Bräuer, A., & Lederer, F. (1999). *Phys. Rev. Lett.*, **83**, 4752.
- [34] Lenz, G., Talanina, I., & de Sterke, C. M. (1999). *Phys. Rev. Lett.*, **83**, 963.
- [35] Lenz, G., Parker, R., Wanke, M. C., & de Sterke, C. M. (2003). *Opt. Comm.*, **218**, 87.
- [36] Wu, B. & Niu, Q. (2000). *Phys. Rev. A*, **61**, 023402.
- [37] Khoo, I. C. & Wu, S. T. (1997). *Optics and Nonlinear Optics of Liquid Crystals*, World Scientific Publ.: Singapore.
- [38] Simoni, F. (1997). *Nonlinear Optical Properties of Liquid Crystals*, World Scientific Publ.: London, UK.
- [39] Dumm, D. A., Fukuda, A., & Luckhurst, G. R. (2001). *Physical Properties of Liquid Crystals: Nematics*, INSPEC: London, UK.
- [40] Assanto, G. & Peccianti, M. (2003). *IEEE J. Quantum Electron.*, **39**, 13.
- [41] Peccianti, M., Conti, C., Assanto, G., de Luca, A., & Umetsu, C. (2004). *Nature*, **432**, 733.
- [42] Fratalocchi, A., Assanto, G., Brzdąkiewicz, K. A., & Karpierz, M. A. (2004). *Opt. Lett.*, **29**, 1530.
- [43] Fratalocchi, A. & Assanto, G. (2005). *Phys. Rev. E*, **72**, 066608.
- [44] Fratalocchi, A., Assanto, G., Brzdąkiewicz, K. A., & Karpierz, M. A. (2005). *Appl. Phys. Lett.*, **86**, 51112.
- [45] Fratalocchi, A., Assanto, G., Brzdąkiewicz, K. A., & Karpierz, M. A. (2005). *Opt. Lett.*, **30**, 174.
- [46] Mandelik, D., Eisenberg, H. S., Silberberg, Y., Morandotti, R., & Aitchison, J. S. (2003). *Phys. Rev. Lett.*, **90**, 053902.